2010 IEEE International Conference on Robotics and Automation
Anchorage Convention District
May 3-8, 2010, Anchorage, Alaska, USA

A Potential Field Approach to Finding Minimum-Exposure Paths in Wireless Sensor Networks

S. Ferrari and G. Foderaro

Abstract— **A novel artificial-potential approach is presented for planning the minimum-exposure paths of multiple vehicles in a dynamic environment containing multiple mobile sensors, and multiple fixed obstacles. This approach presents several advantages over existing techniques, such as the ability of computing multiple minimum-exposure paths online, while avoiding mutual collisions, as well as collisions with obstacles sensed during the motion. Other important advantages include the ability of utilizing heterogenous sensor models, and of meeting multiple objectives, such as minimizing power required, and reaching a set of goal configurations. The approach is demonstrated through numerical simulations involving autonomous underwater vehicles (AUVs) deployed in a region of interest near the New Jersey coast, with ocean currents simulated using real coastal ocean dynamics applications radar (CODAR) data.**

I. INTRODUCTION

Path exposure can be described as the ability of detecting a target moving in a region of interest populated by a wireless sensor network. In [1], exposure was defined as the time integral of the cumulative energy received by all sensors in the network. In [2], a new definition of exposure was introduced pertaining the probability of detection by a cooperative sensor network that arrives at a consensus decision only when the number of detections exceeds a user-defined threshold. In both definitions, each sensor is considered to be omnidirectional, and is modeled by a decaying exponential function of its distance from the target, which represents its received energy. The problem of finding a target path of minimum exposure can then be formulated as a trajectory optimization problem in which the cost function to be minimized is the path exposure. As reviewed in [2], this problem is of concern in a number of applications employing wireless sensor networks for detecting, tracking, and monitoring unauthorized targets traversing a region of interest. As a result, approaches based on calculus of variations and Voronoi diagrams have been proposed in the literature in order to compute a single-target path of minimum exposure in a given sensor network [1], [3], [4].

In this paper, a novel artificial-potential field approach is presented for finding a set of minimum-exposure paths in a given sensor network. Potential field presents several advantages over existing techniques, such as the ability of computing paths online for many targets moving simultaneously through the sensor network, while avoiding mutual collisions and collisions with obstacles detected in the region of interest. By computing paths online, the target paths computed by this approach can minimize exposure to a mobile sensor network, and avoid collisions with obstacles that are sensed while the motion is being executed. Other important advantages include the ability of utilizing heterogenous sensor models, and the ability of meeting multiple simultaneous objectives, such as minimizing power required, and reaching a final goal configuration.

Potential field is an effective path planning technique that was developed and refined in [5]–[8] for the purpose of online obstacle avoidance. Several artificial potential functions have, therefore, been developed to represent the robot's objective of navigating a region of interest to reach a goal configuration, while avoiding collisions with the obstacles. This paper presents an adaptive novel potential function that represents the exposure of any path in the region of interest over time, as well as a novel potential function for minimizing power required in a current velocity field, which is applicable to targets moving in a water body, or in the atmosphere. The approach is demonstrated by planning multiple minimum-exposure paths in a mobile ocean sensor network deployed in a region of interest near the New Jersey coast. The sensors and the targets are simulated using a high-fidelity simulation of an autonomous underwater vehicle described in [9], and using real ocean current data obtained from the Coastal Ocean Observation Lab of Rutgers University [10].

The paper is organized as follows. The minimum-exposure path-planning problem formulation and assumptions are presented in Section II. A review of the background on artificial potential field is provided in Section III, and the novel potential-field methodology for computing minimum-exposure paths is presented in Section IV. The simulation results presented in Section V show that this methodology minimizes a tradeoff of exposure and power required, and computes collision free paths online, subject to a mobile sensor network and fixed obstacles that are sensed while the motion is executed.

II. PROBLEM FORMULATION AND ASSUMPTIONS

Consider a rectangular region of interest (ROI) populated by a field of n mobile sensors deployed at time-varying locations $\mathbf{s}_i(t)$, $i = 1, \ldots, n$, during a time interval $t \in [t_0,\ t_f]$. The i^{th} sensor located at $\mathbf{s}_i(t)$ is modeled by its received energy which is given by,

$$E_i(\mathbf{q}, t) = \frac{K_i}{||\mathbf{q} - \mathbf{s}_i(t)||^{\alpha_i}} + N_i \qquad (1)$$

S. Ferrari and G. Foderaro are with the Laboratory for Intelligent Systems and Control (LISC), Department of Mechanical Engineering and Materials Science, Duke University, Durham, NC 27708-0005, {sferrari, greg.foderaro}@duke.edu

where, K_i and α_i are known positive constants that depend on the sensor and environmental conditions, $\mathbf{q} = [x\ y]^T$ is the target position, and N_i is additive white Gaussian noise (AWGN). Thus, for a target located at $\mathbf{q}$ the total received energy of the sensor network at time t is given by,

$$E_{tot}(\mathbf{q}, t) = \sum_{i=1}^{n} \left[\frac{K_i}{||\mathbf{q} - \mathbf{s}_i(t)||^{\alpha_i}} + N_i \right] \quad (2)$$

and the network declares a consensus target detection when $E_{tot} \geq \theta$ [2]. For simplicity, it is assumed that the sensors' paths and characteristics are known without error at any $t \in [t_0,\ t_f]$. Since the method presented in Section IV uses a time-varying potential function, it can be implemented using real-time estimates of $\mathbf{s}_i(t)$, K_i, and α_i.

The ROI, denoted by $\mathcal{S} = [0,\ L] \times [0,\ L] \subset \mathbb{R}^2$, has a boundary $\partial\mathcal{S}$ and is populated by N fixed and convex obstacles $\{\mathcal{B}_1, \ldots, \mathcal{B}_N\} \subset \mathcal{S}$ that are not necessarily known *a priori*, but may be detected at any time $t \in [t_0,\ t_f]$. This paper develops an approach for computing the minimum-exposure paths for a network of m autonomous underwater vehicles (AUVs) that must traverse $\mathcal{S}$, while all obstacles and mutual collisions. Each AUV in the network is described by the following dynamical model [8], [11].

$$M(\mathbf{q}_j)\ddot{\mathbf{q}}_j + f(\mathbf{q}_j, \dot{\mathbf{q}}_j) + g(\mathbf{q}_j) = u(\mathbf{q}_j),\ j = 1, \ldots, m \quad (3)$$

where $M(\mathbf{q}_j)$ is the robotic sensor's inertia matrix, $f(\mathbf{q}_j, \dot{\mathbf{q}}_j)$ is the fictitious force, $g(\mathbf{q}_j)$ is the gravitational force, and $u(\mathbf{q}_j)$ is the torque input. Although the method can be applied to heterogenous networks, for simplicity in this paper it is assumed that all AUVs obey the same dynamic model.

In many applications, an unauthorized vehicle in a sensor field is detected when the sensors have reached a consensus and their total received energy, E_{tot}, exceeds a value fusion threshold denoted by θ. Therefore, we adapt the definition of exposure from [1], as follows:

Definition 1: The exposure of a path or trajectory $\mathbf{q}_j(t)$ in $\mathcal{S}$ during the interval $[t_0,\ t_f]$ is the total received energy,

$$E[\mathbf{q}_j(t), t_0, t_f] = \int_{t_0}^{t_f} E_{tot}[\mathbf{q}_j(t), t] \left| \frac{d\mathbf{q}_j(t)}{dt} \right| dt \quad (4)$$

where $|d\mathbf{q}_j/dt|$ is the element of arc length, and $E_{tot}(\cdot)$ is given by (2).

Since the AUV is subject to the ocean currents, its velocity in inertial frame is $\dot{\mathbf{q}}_j = \boldsymbol{\nu}_j + \boldsymbol{\upsilon}_j$, where $\boldsymbol{\nu}_j \in \mathbb{R}^2$ is the velocity vector in body coordinate frame (fixed to the vehicle), and $\boldsymbol{\upsilon}_j \in \mathbb{R}^2$ is the local current velocity vector. As shown in [12]–[15], the instantaneous AUV's power required is proportional to $\boldsymbol{\nu}_j \in \mathbb{R}^2$, and can be approximated by the quadratic cost,

$$e[\boldsymbol{\nu}_j(t)] = \boldsymbol{\nu}_j^T(t)\mathbf{R}\boldsymbol{\nu}_j(t) \quad (5)$$

in order to penalize large power dissipations more heavily than small dissipations [16, pg.190]. Where, $\mathbf{R} \in \mathbb{R}^{2\times 2}$ is a diagonal weighting matrix with elements that represent the relative importance of velocity components. In this paper, all components are considered equivalent, and thus $\mathbf{R} = \mathbf{I}_2$, where $\mathbf{I}_2$ is a 2×2 identity matrix. The power required by the network of AUVs during the interval $[t_0,\ t_f]$ is then modeled by the integral cost,

$$\mathcal{E}[\dot{\mathbf{q}}_j(t), t_0, t_f] = \int_{t_0}^{t_f} \sum_{j=1}^{m} [\dot{\mathbf{q}}_j(t) - \boldsymbol{\upsilon}_j(t)]\ \mathbf{I}_2 [\dot{\mathbf{q}}_j(t) - \boldsymbol{\upsilon}_j(t)] dt \quad (6)$$

where, $\boldsymbol{\upsilon}_j(t)$ can be estimated from the forecast models of the ocean dynamics, and on-line measurements, as explained in Section IV.

The path exposure problem considered in this paper can be summarized as follows:

Problem 2.1: Exposure in Multi-Target Multi-Sensor Networks. Given on-line information about the ROI, $\mathcal{W}$, containing N fixed and convex obstacles $\{\mathcal{B}_1, \ldots, \mathcal{B}_N\}$ and n mobile sensors with received energy (1), find a set of minimum-exposure paths, $\mathcal{P} = \{\mathbf{q}_1(t), \ldots, \mathbf{q}_m(t)\}$, for a network of m AUVs that minimize the power required (6), and avoid collisions in $\mathcal{W}$ during the interval $[t_0,\ t_f]$.
The methodology for computing $\mathcal{P}$, presented in Section IV, is based on the potential field approach reviewed in the next section.

III. BACKGROUND ON POTENTIAL FIELD METHODS

Potential field is well-known approach to robot motion planning that treats the robot as a particle under the influence of an artificial potential field or function, U, that captures the geometric characteristics of the workspace or ROI, $\mathcal{W}$. So far, several potential field methods have been developed for generating a collision-free path for a robot that must travel from an initial configuration $\mathbf{q}_0$ to a goal configuration $\mathbf{q}_f$, without a prior model of the obstacles. The advantage of potential field over other motion planning approaches, such as, cell decomposition and probabilistic roadmap methods, is that it can easily account for obstacles that are sensed *online*, i.e., during the motion execution [5]. Since the robot follows the direction of steepest descent, however, it can potentially get stuck at a local minimum of U. In this case, the method can be combined with a graph searching technique, or a random-walk algorithm, to help the robot escape local minima.

Several potential functions have been proposed in the literature to generate U, such that the robot can be guaranteed to reach $\mathbf{q}_f$, while effectively avoiding obstacles in $\mathcal{W}$ [6]–[8]. Typically, the potential function is the sum of an attractive potential U_{att} that "pulls" the robot toward $\mathbf{q}_f$, and a repulsive potential U_{rep} that "pushes" robot away from the obstacles, i.e.:

$$U(\mathbf{q}) = U_{att}(\mathbf{q}) + U_{rep}(\mathbf{q}) \quad (7)$$

The method is implemented by discretizing the robot workspace obtained by the Cartesian product, $\mathcal{A} \times \mathcal{C} \to \mathcal{W}$, between the robot geometry $\mathcal{A}$, and the configuration space $\mathcal{C}$. The potential function is evaluated for all $\mathbf{q} \in \mathcal{C}$, using a finite resolution grid [17] which, in on-line motion planning, can be limited to the neighborhood of the configuration at

the present time t. Subsequently, at any time $t \in [t_0,\ t_f]$, an artificial force $\mathbf{F}(\mathbf{q})$ that is proportional to the negative gradient of the artificial potential, $-\nabla U(\mathbf{q})$, is applied to the robot, in order to follow the steepest-descent direction of U.

Every obstacle $\mathcal{B}_i$ in $\mathcal{W}$ maps in $\mathcal{C}$ to a C-obstacle that is defined as the subset of $\mathcal{C}$ that causes collisions with $\mathcal{B}_i$, i.e., $\mathcal{CB}_i \equiv \{\mathbf{q} \in \mathcal{C} \mid \mathcal{A}(\mathbf{q}) \cap \mathcal{B}_i \neq \emptyset\}$, where $\mathcal{A}(\mathbf{q})$ denotes the subset of $\mathcal{W}$ occupied by the platform geometry $\mathcal{A}$ when the robot is in the configuration $\mathbf{q}$. The union of all C-obstacles in $\mathcal{W}$ is referred to as the C-obstacle region. Thus, to avoid collision, the robot is free to explore the free configuration space, defined as the complement of the C-obstacle region $\mathcal{CB}$ in $\mathcal{C}$, i.e., $\mathcal{C}_{free} = \mathcal{C} \backslash \mathcal{CB}$ [5]. As shown in [5], the repulsive potential for a set of obstacles $\{\mathcal{B}_1, \ldots, \mathcal{B}_N\}$ can be defined as,

$$U_{rep}(\mathbf{q}) = \begin{cases} \frac{1}{2}\eta(\frac{1}{\rho(\mathbf{q})} - \frac{1}{\rho_0})^2 & \text{if} \quad \rho(\mathbf{q}) \leq \rho_0 \\ 0 & \text{if} \quad \rho(\mathbf{q}) > \rho_0 \end{cases} \tag{8}$$

where, $\rho(\mathbf{q})$ is the distance from $\mathbf{q}$ to $\mathcal{CB}$,

$$\rho(\mathbf{q}) = \min_{\mathbf{q}' \in \mathcal{CB}} \|\mathbf{q} - \mathbf{q}'\|, \quad \mathcal{CB} \equiv \cup_{i=1}^{N} \mathcal{CB}_i \tag{9}$$

$\eta > 0$ is a scaling factor, and $\rho_0 > 0$ is a distance-of-influence parameter that is chosen by the user. The attractive potential is given by,

$$U_{att}(\mathbf{q}) = \frac{1}{2}\varepsilon \rho_{goal}^2(\mathbf{q}) \tag{10}$$

where $\varepsilon > 0$ is a scaling factor, and $\rho_{goal}(\mathbf{q})$ is the distance between the robot and $\mathbf{q}_f$. By this approach, only the obstacle closest to $\mathbf{q}$ is considered in $U_{rep}(\mathbf{q})$, and the goal configuration is assumed to be a single point in $\mathcal{C}_{free}$.

In the following section, a novel time-varying potential function is presented that captures the robot exposure to a heterogeneous sensor network, as well as the geometric characteristics of multiple obstacles in $\mathcal{W}$ that may be moving or may be sensed on line, during path execution.

IV. POTENTIAL FIELD METHOD FOR MINIMUM-EXPOSURE PATH PLANNING

A potential field approach to solving Problem 2.1 is presented in this section, and demonstrated through numerical simulations involving a network of AUVs in a dynamic ocean environment in Section V. The approach consists of generating a novel potential function that differs from those previously presented in the literature in that it is time-varying, it is applicable to multiple robotic targets and multiple obstacles, and captures the geometric characteristics of the targets' exposure to a mobile sensor network, and of the power required to navigate a known velocity field. For simplicity, it is assumed that each AUV is a point mass, and thus $\mathcal{C} = \mathcal{W}$. However, the method can be easily extended to account for a finite geometry $\mathcal{A}$ by computing the C-obstacle region, as described in Section III.

Collisions between the m targets (AUVs) are avoided by introducing a repulsive potential that target j must follow to avoid collisions with target ℓ,

$$U_{\ell_{rep}}(\mathbf{q}_j, t) = \begin{cases} \frac{1}{2}\eta\left(\frac{1}{\rho_{\ell j}(\mathbf{q}_j,t)} - \frac{1}{\rho_0}\right)^2 & \text{if} \quad \rho_{\ell j}(\mathbf{q}_j,t) \leq \rho_0 \\ 0 & \text{if} \quad \rho_{\ell j}(\mathbf{q}_j,t) > \rho_0 \end{cases} \tag{11}$$

where $\rho_{\ell j}$ is the Euclidian distance between the j^{th} target and the nearest ℓ^{th} target at time t, defined as,

$$\rho_{\ell j}(\mathbf{q}_j, t) = \min_{\mathbf{q}_\ell} \|\mathbf{q}_j(t) - \mathbf{q}_\ell(t)\|, \quad \ell = 1, \ldots, m, \quad \ell \neq j \tag{12}$$

and the other quantities are defined as in Section III.

Collisions with a set fixed obstacles $B(t) \equiv \{\mathcal{B}_1, \mathcal{B}_2, \ldots\}$ in $\mathcal{W}$ that are sensed online at or before t are avoided by means of an additive repulsive potential that can be easily updated as new obstacles are sensed during $[t_0,\ tf]$ [18]. Let $U_{i_{obs}}(\mathbf{q}_j, t)$ represent the repulsive potential for target j that is generated by the ith obstacle sensed at or before time t. Where, $U_{i_{obs}}$ is computed from (8)-(9), by letting $\mathbf{q} = \mathbf{q}_j(t)$, and $\mathbf{q}' \in \mathcal{CB}_i$. Then, the repulsive function for the C-obstacle region at time $t \in [t_0,\ tf]$ is,

$$U_{obs}(\mathbf{q}_j, t) = \sum_i U_{i_{obs}}(\mathbf{q}_j, t), \quad \forall \mathcal{B}_i \in B(t) \tag{13}$$

where, $i = 1, \ldots, m' < m$.

The artificial potential presented in this paper has no attractive component, although one could be included in case the targets need to reach a set of goal configurations. Instead, two new potentials are included in order to minimize the power required and the exposure to the sensor network. First, consider the power required in (6), which is proportional to the AUV's velocity vector in body coordinate frame. As shown in [19], the influence of ocean currents on the AUV's motion can be modeled in order to exploit the natural dynamics for AUVs' transport and minimize the power required. A forecast of the ocean current field can be computed from a physical model of the ocean initialized with real-time measurements and estimates of the currents [20], using state-estimation techniques [21], [22]. This forecast, denoted by $\mathcal{F}$, consists of a multi-dimensional array containing estimated values of $\boldsymbol{\upsilon}_j$ at sample points in space and time. The approach presented in [19] obtains from $\mathcal{F}$ a smooth functional representation of the forecasted current velocity field over $\mathcal{W}$, for a future time interval.

Let $\boldsymbol{\eta}_j(t) \equiv [\mathbf{q}_j^T(t)\ \ t]^T \in \mathcal{N}$, where $\mathcal{N} = \mathcal{W} \times [t_0,\ t_f]$. The current forecast $\mathcal{F} = \{\mathbf{q}_j^\kappa, \boldsymbol{\upsilon}_i^\kappa, t^\kappa\}_{\kappa=1,\ldots,p}$ contains the value $\boldsymbol{\upsilon}_i^\kappa$ of the local current velocity vector at the configuration $\mathbf{q}_j^\kappa$, and at time t^κ, for p sample points in $\mathcal{N}$. Then, $\mathcal{F}$ can be considered as the training set of a feedforward neural network,

$$\boldsymbol{\upsilon}_j[\mathbf{q}_j(t), t] = \mathbf{W}_2 \boldsymbol{\Phi}[\mathbf{W}_1\ \boldsymbol{\eta}(t) + \mathbf{b}_1] + \mathbf{b}_2 \tag{14}$$

with two linear output neurons, and one hidden layer of s sigmoidal functions represented by the operator $\boldsymbol{\Phi}(\mathbf{n}) \equiv [\sigma(n_1)\ \cdots\ \sigma(n_s)]^T$, where $\sigma(n_i) \equiv 1/(1 + e^{-n_i})$. As shown in [19], the weights $\mathbf{W}_1 \in \mathbb{R}^{s \times 3}$, $\mathbf{W}_2 \in \mathbb{R}^{2 \times s}$, $\mathbf{b}_1 \in \mathbb{R}^s$, and $\mathbf{b}_2 \in \mathbb{R}^2$, can be determined from $\mathcal{F}$ by a

Bayesian regularization backpropagation algorithm ('trainbr' [23]). The effectiveness of the approach has been verified in [19] through numerical experiments with real measurements.

It was recently in [12], [13], [19], [24] that the total power required (5) can be minimized by computing AUVs' trajectories that account for the local current velocity vector $\boldsymbol{\upsilon}_j$ estimated from $\mathcal{F}$. As can be expected, minimum-energy trajectories utilize knowledge of the ocean's velocity field, thereby minimizing deviations from the trajectories of Lagrangian fluid particles in an irrotational flow with a vector field given by the model (14). The ocean flow velocity $\boldsymbol{\upsilon}_j$ is a vector field that is equal to the negative gradient of the velocity potential φ, i.e., $\boldsymbol{\upsilon}_j = -\nabla\varphi$ [25]. It follows that the power required by the jth target can be minimized by including an attractive potential given by the potential flow corresponding to ocean current forecast $\mathcal{F}$.

In order to minimize exposure and avoid collisions with minimum energy consumption, the artificial potential function for target j is defined as,

$$\begin{aligned} U(\mathbf{q}_j,t) &= w_E\ E_{tot}(\mathbf{q}_j,t) + \sum_{\ell=1,\ell\neq j}^{m} U_{\ell_{rep}}(\mathbf{q}_j,t) \\ &+ U_{obs}(\mathbf{q}_j,t) + w_{\mathcal{E}}\ \varphi[\mathbf{q}_j(t),t], \quad \forall t\in[t_0,t_f] \end{aligned} \tag{15}$$

where $w_E, w_{\mathcal{E}} > 0$ are constant weights chosen by the user based on the desired tradeoff between the exposure and energy objectives, and every potential component is defined as shown in (11)-(13). Although the velocity potential may be computed by integrating (14), in practice it is never needed because the paths of the AUVs are computed from the gradient of U.

According to the potential field approach, the force applied to target j is proportional to the negative gradient of U at t,

$$\mathbf{F}(\mathbf{q}_j,t) = -\nabla U(\mathbf{q}_j,t) = -\left[\frac{\partial U(\mathbf{q}_j,t)}{\partial x_j} \cdots \frac{\partial U(\mathbf{q}_j,t)}{\partial y_j}\right]^T \tag{16}$$

where $\mathbf{q}_j = [x_j \quad y_j]^T$. However, in this paper, every AUV (target) j is assumed to move in the workspace with a constant speed relative to a fixed point. This is achieved by using the constant speed value as a reference for a PID controller that returns the appropriate propeller rotational speed to compensate for a changing ocean flow velocity, v_j. Since the speed of target j in the workspace is independent of $\mathbf{F}(\mathbf{q}_j,t)$, the gradient of the potential U is only used to determine the optimal heading angle of the AUV. Target j adjusts to the heading angle by using it as a reference for a second PID controller that computes a rudder position. In future work, the method will be further improved such that the artificial potential in (15) may be used directly to compute the input to the AUV. For example, the following time-varying feedback control law,

$$u = -\nabla U(\mathbf{q}_j,t) + d(\mathbf{q}_j,\dot{\mathbf{q}}_j) \tag{17}$$

where $d(\mathbf{q},\dot{\mathbf{q}})$ is an arbitrary dissipative force, may be adapted from [8], and applied to the jth AUV with dynamic equation (3) for inner-loop control.

V. SIMULATIONS AND RESULTS

The methodology presented in the previous section is demonstrated here on a simulated ocean sensor network comprised of $n = 12$ sensors, $m = 5$ targets and $N = 3$ static obstacles deployed at arbitrary positions in a ROI, $\mathcal{S} = [0,\ L_1] \times [0,\ L_2]$ where $L_1 = 90\ km$ and $L_2 = 82.51\ km$. The simulation was run over the time interval $t \in [t_0\ tf]$ in increments of $t_s = 1$ sec with $t_0 = 0$ and $t_f = 8$ hr. The sensors' trajectories were chosen as arbitrary linear paths across the ROI. The coefficients K_i and α_i were chosen as 10 and 2 respectively for all sensors, and N_i was modeled in MATLAB using the function 'awgn' [2]. The repulsive potential constants η and ρ_0 were chosen as 200 and 5 km, respectively. Identical repulsive potentials were applied to target vehicles, static obstacles and the boundaries of $\mathcal{S}$. The time-varying ocean current velocity field within $\mathcal{S}$ was generated from the feedforward neural network (14) and CODAR data given by COOL at Rutgers University [10]. A snapshot of the velocity field is shown in Figure 1.

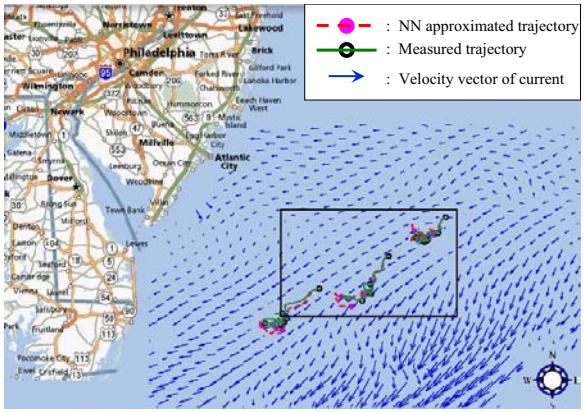

Fig. 1. Example ocean current velocity field obtained from the neural network and from CODAR measurements in ROI $\mathcal{S}$ (black rectangle) with longitude of 72.7° W to 74.1° W, and a latitude of 38.6° N to 39.5° N (taken from [19]). t = 4.0 hr.

The dynamic equation (3) was simulated using a high-fidelity simulation of the REMUS 100 AUV (described in [9]), obtaining the AUV state over time. For every state value, the simulation implements two proportional-integral-derivative (PID) controllers to calculate the vehicle propeller rotational speeds and rudder angles based on the desired heading angles and speeds. In this paper, since the paths $\mathcal{P}$ are produced by the potential function approach described in Section IV, the desired heading angles are computed from the optimal directions of movement in $\mathcal{P}$. In particular, the gradient of $U(\mathbf{q}_j,t)$ is computed by evaluating all of the potentials at several points around $\mathbf{q}_j$. The 'gradient' function in MATLAB can also be used for this purpose. The desired speeds were set to be constant at 2.0 m/s relative to a fixed point, but the vehicle speeds relative to the ocean current velocities, and therefore the propeller rotational speeds, were continuously changed depending on the ocean movements at the AUVs' positions. Figure 2 shows the AUVs' state values at several instants during the simulation

with the resulting headings of the targets. The potential field evaluated from (15) is illustrated in the background of Fig. 2, and in Fig. 4, and the targets are seen to continuously move down the slopes as they follow the potential field gradients. Figure 3 represents the received sensor energies for the same vehicle positions and shows how the effectiveness of the sensors is high within a certain range but rapidly decreases at further distances. The full AUVs' trajectories are also plotted.

The effectiveness of this methodology is shown by evaluating performance metrics (exposure, power required, and number of sensor detections) and comparing them to the those obtained using alternate strategies. The method presented in this paper, labeled as Potential Field in Table I, uses the technique discussed in Section IV and generates paths for the targets that minimize the exposure and power required while also avoiding obstacles. The strategy Minimum Energy finds paths that avoid obstacles and minimize the power required. The method Obstacle Avoidance instructs the targets to move in linear trajectories towards arbitrary goal positions only altering their paths to travel around obstacles. Each technique was implemented in 5 simulations with $n = 12$ sensors, $m = 5$ targets and $N = 3$ static obstacles in the ROI, $\mathcal{S}$ over the time interval $t \in [t_0\ tf]$ in increments of $t_s = 1$ sec with $t_0 = 0$ and $t_f = 6$ hr. The vehicles and obstacles were given random initial and goal positions. The results are averaged and displayed in Table I with a sensor detection of target j defined as an event in which $E_{tot}(\mathbf{q}_j, t) \geq \theta$ where $\theta = 1$ for a single target. Each target vehicle was limited to one recorded detection per simulation, and the maximum exposure per target at any instant was bounded to 1.5 since it asymptotically approaches infinity near the sensor. It can be seen that Minimum Energy requires the least power but has very high exposure. Potential Field sacrifices some movement efficiency to minimize exposure and, thus, it drastically decreases the number of detections per path. The user may tune the tradeoff between exposure and energy consumption through the weights w_E and $w_{\mathcal{E}}$.

TABLE I
PERFORMANCE COMPARISON

Performance Metric	Potential Field	Minimum Energy	Obstacle Avoidance
Exposure	$3.4{\cdot}10^{3}$	$6.6{\cdot}10^{3}$	$6.4{\cdot}10^{3}$
Power Required	$4.1{\cdot}10^{-1}$	$3.8{\cdot}10^{-1}$	$4.2{\cdot}10^{-1}$
Sensor Detections	0.6	4.0	4.0

VI. CONCLUSIONS AND FUTURE WORK

This paper presents a novel artificial-potential approach for planning the minimum-exposure paths of multiple AUVs in an ROI containing multiple mobile sensors. The approach presents several advantages over existing calculus-of-variations and Voronoi-diagrams techniques, such as the ability of computing multiple minimum-exposure paths online, while avoiding mutual collisions and collisions with obstacles sensed during the motion. The novel exposure-based po-

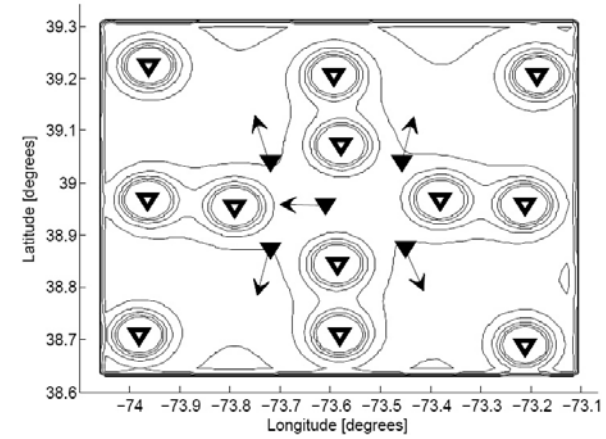

(a)

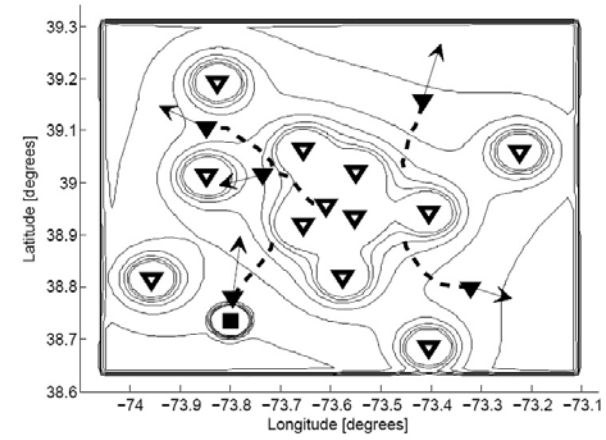

(b)

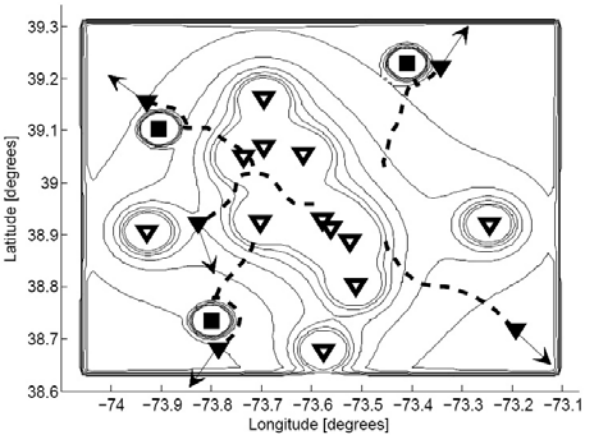

(c)

Fig. 2. Potential field contour plot and target paths for five targets (solid black triangles), twelve sensors (white triangles with black borders), three fixed obstacles (black squares), with targets' heading angles illustrated by vectors, and paths illustrated by dotted lines at (a) t = 0.1 hr, (b) t = 2.5 hr, and (c) t = 4.0 hr.

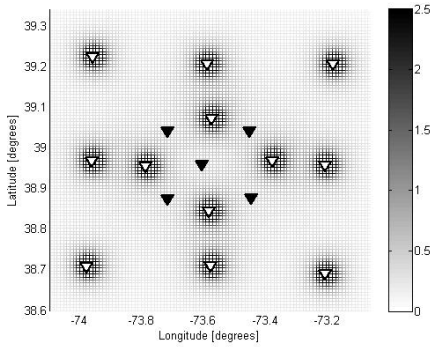

(a)

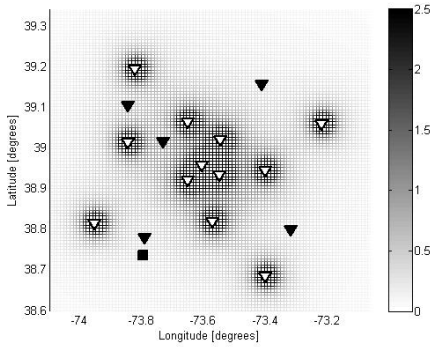

(b)

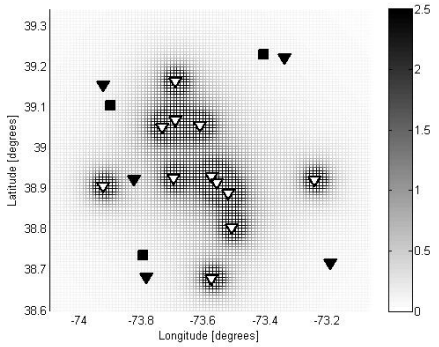

(c)

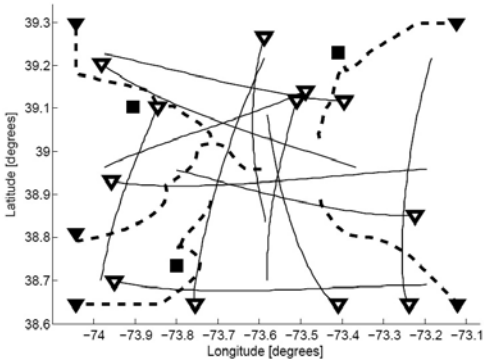

(d)

Fig. 3. Received sensor energy and generated target paths. solid black triangles: targets; white triangles with black outlines: sensors; solid black squares: static obstacles; dotted lines: targets' generated paths; solid lines: sensors' paths. (a) $t = 0.1$ hours, (b) $t = 2.5$ hours, (c) $t = 4.0$ hours, (d) paths of all AUVs after $t = t_f$ hours.

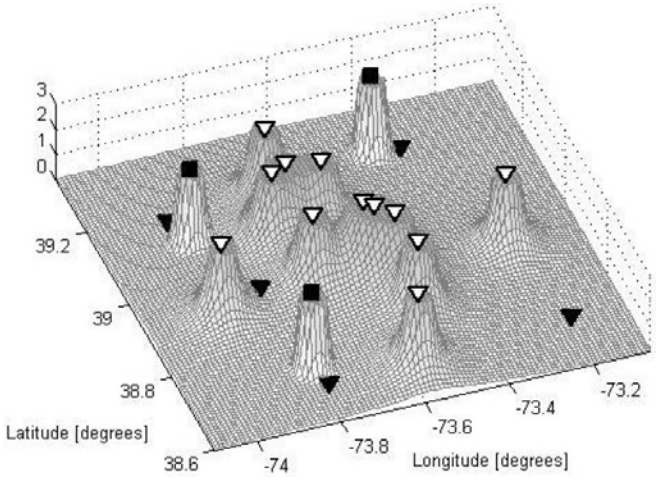

Fig. 4. Example of artificial-potential field (with repulsive potential from boundary omitted) at t = 4.0 hr.

tential function presented in Section IV is augmented with a novel potential-flow component that minimizes energy based on an available forecast of current velocities in the ROI. The numerical simulations presented in Section V, involving a network of autonomous underwater vehicles (AUVs) deployed in a dynamic ROI near the New Jersey coast, show that the approach can be successfully implemented to minimize a desired tradeoff between energy consumption and path exposure, thereby significantly reducing the number of sensor detections over time.

VII. ACKNOWLEDGMENTS

This work was supported by the Office of Naval Research (Code 321).

REFERENCES

[1] S. Megerian, F. Koushanfar, G. Q. amd G. Veltri, and M. Potkonjak, "Exposure in wireless sensor networks: Theory and practical solutions," *Wireless Networks*, vol. 8, pp. 443–454, 2002.

[2] V. Phipatanasuphorn and P. Ramanathan, "Vulnerability of sensor networks to unauthorized traversal and monitoring," *IEEE Transactions on Computers*, vol. 53, no. 3, 2004.

[3] T. Clouqueur, V. Phipatanasuphorn, P. Ramanathan, and K. Saluja, "Sensor deployment for detection of targets traversing a region," *Mobile Networks and Applications*, vol. 8, pp. 453–461, August 2003.

[4] Q. Huang, "Solving an open sensor exposure problem using variational calculus," Washington University, Department of Computer Science, St. Louis, MO, Tech. Rep. WUCS-03-1. [Online]. Available: http://www.cs.wustl.edu/ qingfeng/papers/ExposureTRShort.pdf

[5] J. C. Latombe, *Robot Motion Planning*. Kluwer Academic Publishers, 1991.

[6] J. Ren and K. Mclsaac, "A hybird-systems approach to potential field navigation for a multi-robot team," in *Proc. of IEEE International Conference on Robotics and Automation*, Taipei, Taiwan, 2003, pp. 3875–3880.

[7] S. Shimoda, Y. Kuroda, and K. Iagnemma, "Potential field navigation of high speed unmanned ground vehicles on uneven terrain," in *Proc. of IEEE International Conference on Robotics and Automation*, Barcelona, Spain, 2005, pp. 2839–2844.

[8] S. Ge and Y. Cui, "New potential functions for mobile robot path planning," *IEEE Transactions on Robotics and Automation*, vol. 16, no. 5, 2000.

[9] A. Shcherbina, G. Gawarkiewicz, C. Linder, and S. Thorrold, "Mapping bathymetric and hydrographic features of glovers reef, belize, with a remus autonomous underwater vehicle," *Limnology and Oceanography*, vol. 53, no. 5, pp. 2264–2272, 2008.

[10] (2002) COOL, Rutgers University. [Online]. Available: http://marine.rutgers.edu/
[11] E. Rimon and D. Kodischek, "Exact robot navigation using artificial potential functions," *IEEE Transactions on Robotics and Automation*, vol. 8, no. 5, 1992.
[12] A. Alvarez, A. Caiti, and R. Onken, "Evolutionary path planning for autonomous underwater vehicles in a variable ocean," *IEEE Journal of Oceanic Engineering*, vol. 29, no. 2, pp. 418–429, 2004.
[13] T. Inanc, S. C. Shadden, and J. E. Marsden, "Optimal trajectory generation in ocean flows," in *Proceedings of the 2005 American Control Conference*, Portland, OR.
[14] I. Spangelo and O. Egeland, "Trajectory planning and collision avoidance for underwater vehicles using optimal control," *IEEE Journal of Oceanic Engineering*, vol. 19, no. 4, pp. 502–511, 1994.
[15] P. van de Ven, C. Flanagan, and D. Toal, "Neural network control of underwater vehicles," *Detection and Remediation Technologies for Mines and Minelike Targets VIII, Proc. of the SPIE*, vol. 18, no. 5, pp. 533–547, 2005.
[16] R. F. Stengel, *Optimal Control and Estimation*. Dover Publications, Inc., 1986.
[17] J. Barraquand, B. Langlois, and J.-C. Latombe, "Numerical potential field techniques for robot path planning," *IEEE Transactions on Systems, Man, and Cybernetics*, vol. 22, no. 2, 1992.
[18] G. Zhang and S. Ferrari, "An adaptive artificial potential function approach for geometric sensing," in *Proc. of the IEEE Conference on Decision and Control*, Shanghai, China, 2010, p. in press.
[19] K. C. Baumgartner, S. Ferrari, and T. Wettergren, "Robust deployment of dynamic sensor networks for cooperative track detection," *IEEE Sensors*, vol. in press, 2009.
[20] A. Liu, Y. Zhao, and M.-K. Hsu, "Ocean surface drift revealed by synthetic aperture radar images," *EOS*, vol. 87, no. 24, pp. 233–239, 13 June 2006.
[21] A. R. Robinson, "Physical processes, field estimation and an approach to interdisciplinary ocean modeling," *Earth-Science Reviews*, vol. 40, pp. 3–54, 1996.
[22] P. F. J. Lermusiaux, "Evolving the subspace of the three-dimensional multiscale ocean variability: Massachusetts bay," *Journal of Marine Systems*, vol. 29, 2001.
[23] Mathworks, *MATLAB Neural Network Toolbox*. [Online]. Avaliable: http://www.mathworks.com, 2006, function: trainbr.
[24] F. Lekien, C. Coulliette, R. Bank, and J. Marsden, "Open-boundary modal analysis: Interpolation, extrapolation and filtering," *Journal of Geophysical Research - Oceans*, vol. 109, no. C12, 2004.
[25] H. Lamb, *Hydrodynamics*. Cambridge University Press, 1994.